https://doi.org/10.5194/egusphere-2023-2316
Preprint. Discussion started: 24 October 2023

Hydrogen solubility of stishovite provides insights into water transportation to deep Earth

Mengdan Chen[1], Changxin Yin[1], Danling Chen[1], Long Tian[1], Liang Liu[1], and Lei Kang[1]

[1]Department of Geology, Northwest University/State Key Laboratory of Continental Dynamics, Xi'an, 710069, China

Correspondence to: Lei Kang (kanglei@nwu.edu.cn); Liang Liu (liuliang@nwu.edu.cn)

Abstract. Water dissolved in nominally anhydrous minerals (NAMs) can be transported to deep regions of the Earth through subducting slabs, thereby significantly influencing the physicochemical properties of deep Earth materials and impacting dynamic processes in the deep Earth. Stishovite, a prominent mineral found in subducting slabs, remains stable at mantle conditions ranging from pressure of 9-50 GPa and can incorporate varying amounts of water (H^+, OH^-, and H_2O) within its crystal structure. Consequently, stishovite plays a crucial role in transporting water into deep Earth through subducting slabs. This paper provides a comprehensive review of the research progress concerning water (hydrogen) solubility in stishovite. The key factors that govern water solubility in stishovite are summarized as temperature, pressure, water fugacity and aluminum content. Combined with published results on the dependence of water solubility on the aforementioned parameters, this paper proposes a new equation for water solubility in Al-bearing stishovite can be described by the relationship. Calculation results based on this equation suggest that stishovite may effectively absorb water released from processes such as hydrous mineral breakdown, dehydration reactions, and volume reduction, ultimately contributing to the presence of a water-rich transition zone.

1 Introduction

Water plays a crucial role not only in the origin and evolution of life but also in various Earth processes, including slab subduction, crust-mantle reaction and recycling. During slab subduction, water is transported from the Earth's surface to its interior through subduction zones, and a significant amount of water returns to the surface mainly through magmatism, thus forming a large-scale water cycle (Fig. 1). In subducting slabs, water exists both explicitly and implicitly. Explicit water components include H_2O, OH^- and H^+ in melts, fluids, fluid inclusions, and hydrous minerals such as amphibole and mica (Johnson, 2006; Libowitzky, 2006; Litasov and Ohtani, 2007). Implicit water primarily occurs as hydroxyl (OH^-) in nominally anhydrous minerals (NAMs) at defects in crystal structures (Bell et al., 1995; Rossman, 1996; Xia et al., 1998). Most hydrous minerals in subducting slabs decompose and release water before reaching a depth of 300 km (Poli and Schmidt, 2002). Part of this water returns to the surface through magmatism, while the remainder is incorporated into NAMs in ultrahigh-pressure metamorphic rocks(Magni et al., 2014; Walter, 2021) and subsequently transported to deep mantle by subducting slabs (Ishii et al., 2022).

https://doi.org/10.5194/egusphere-2023-2316
Preprint. Discussion started: 24 October 2023

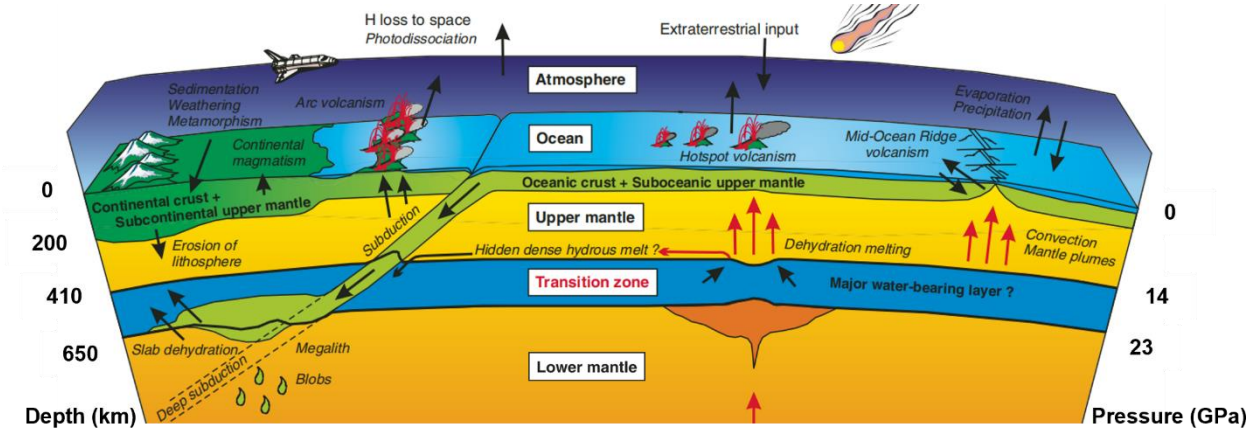

Figure 1: Water transport, distribution, and cycling in the Earth (after Litasov and Ohtani, 2007)

Numerous studies indicate that major constituent minerals in deep mantle, such as olivine, pyroxene, and garnet, as well as their high-pressure polymorphs, are NAMs (Litasov and Ohtani, 2007; Liu et al., 2016). Although the phase of SiO_2 does not typically appear in the mantle (Kaminsky, 2012) (Fig. 2), it is a significant constituent mineral in silica-riched slabs and can stably exist at upper to lower mantle depths through high-pressure polymorphic phase transitions. Both experimental and computational studies have demonstrated that stishovite's crystal structure can incorporate a certain amount of water. Given its prevalence as a major mineral in subducting slabs at mantle depths (>300 km), stishovite likely plays a significant role in water transport to deep earth (Spektor et al., 2011; Lin et al., 2022; Ishii et al., 2022). In this paper, we provide a systematic review of previous understandings and research progress regarding water solubility, water incorporation mechanisms, and factors influencing water solubility in stishovite. Combined with published results, we establish an empirical model for water solubility in Al-stishovite, and discuss the significance of stishovite in transporting water from subducting slabs to the deep mantle and its implications for deep Earth dynamics. Finally, we highlight key unresolved scientific questions in the research on water solubility in stishovite.

2 Crystal structure and stability of stishovite

Phase of SiO_2 undergoes multiple high-pressure polymorphic transitions as pressure increases (Petersen et al., 2021) (Fig. 3). Under average geothermal gradient, coesite is the dominant phase of SiO_2 at pressures ranging from 2.7 to 9 GPa. At approximately 10 GPa, coesite transforms into the denser stishovite (Ono et al., 2017). The transition pressure from coesite to stishovite is dependent on temperature, as described by the equation P (GPa) = 4.7 + 0.0032 × T (K) (Ono et al., 2017). This phase transition is believed to contribute to the seismic discontinuity observed at around 300 km depth (Ono et al., 2017). As pressure increases further to 23-50 GPa, stishovite undergoes a transformation into the $CaCl_2$-type SiO_2 structure (Pnnm), commonly referred to as post-stishovite.

https://doi.org/10.5194/egusphere-2023-2316
Preprint. Discussion started: 24 October 2023

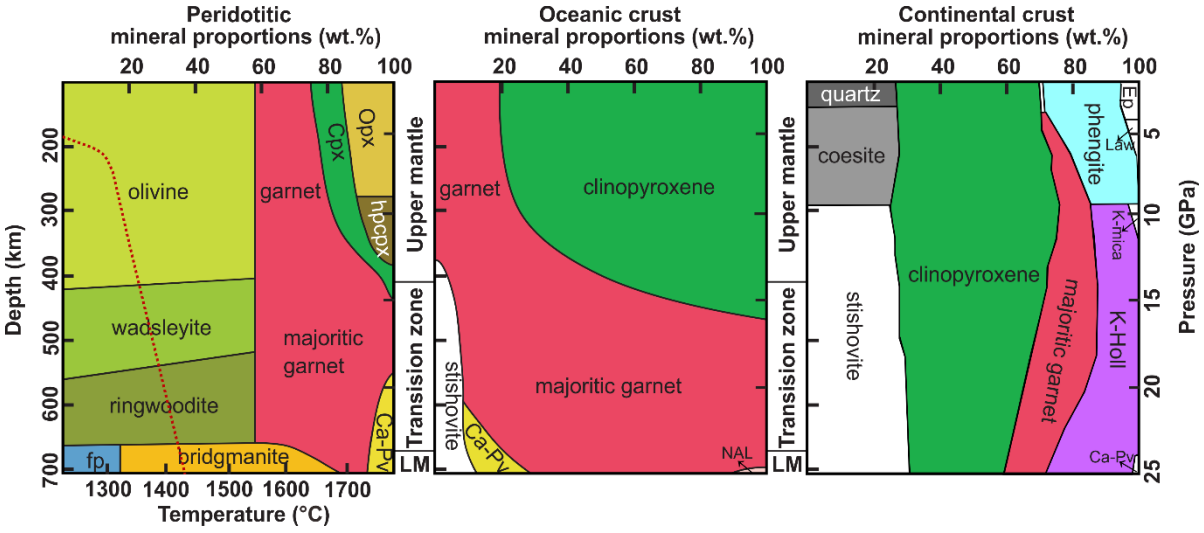

Figure 2: Mantle mineral assemblages in peridotite, subducted oceanic crust, and subducted continental crust. The red line indicates the geotherm. Modified after Smith et al., 2018 and Wu et al., 2009. (Fp—Ferropericlase; Opx—Orthopyroxene; Cpx—Clinopyroxene; Ca-pv—Ca-perovskite; NAL—Na-Al phase; Ep—Epidote; Law—lawsonite; K-Holl—K-Hollandite)

Previous studies show that stishovite constitutes 10 vol. % and 20 vol. % of subducting ocean ridge basalt (MORB) in the upper and lower mantle, respectively (Irifune et al. 1986; Ono et al., 2001). In subducted continental crust at upper mantle depth (<660 km), stishovite can reach approximately 20-25 vol. % (Irifune et al., 1994; Poli and Schmidt, 2002; Ishii et al., 2012). However, due to the exhumation of subducted slabs from ~300 km depth (referred as "depth of no return" in literatures, e.g., Irifune et al., 1994; Liu et al., 2007; Wu et al., 2009) to the surface is extremely difficult, and/or the preservation conditions of stishovite are very harsh, naturally formed stishovite that can be found is extremely rare. Previously, the micro-exsolution structure (Liu et al., 2007) and pseudomorphs after stishovite (Liu et al., 2018) were only found in the South Altyn ultra-high pressure metamorphic belt in western China. Recently, Thomas et al. (2022) identified coesite and stishovite inclusions in Waldheim granulite. In addition, other naturally occurring stishovite is found sporadically in meteorite impact craters (e.g., Chao et al., 1962) or meteorites (e.g., Holtstam et al., 2003). Therefore, the current research on stishovite mainly relies on high-temperature and high-pressure experiments and theoretical calculations (e.g., Litasov et al., 2007; Lin et al., 2022; Ishii et al., 2022).

Stishovite was first synthesized by Stishov and Popova (1961) at 20 GPa (equivalent to approximately 600 km depth in Earth's interior) and 1100℃ from α-quartz. It possesses a rutile-type structure with tetragonal symmetry ($P4_2/mnm$). The Si atoms are coordinated by six O atoms in octahedral arrangements (Pawley et al. 1993; Spektor et al., 2011; Lin et al., 2022). These SiO_6 octahedra align and form linear chains along the c-axis. This arrangement results in a highly dense packing of O atoms, with slightly elongated Si-O bonds compared to SiO_4 tetrahedra. Previous studies have demonstrated that the density of stishovite is 46% higher than coesite and 60% higher than α-quartz (Keskar et al., 1991). Therefore, the formation of

https://doi.org/10.5194/egusphere-2023-2316
Preprint. Discussion started: 24 October 2023

stishovite during slab subduction at depths exceeding 300 km increases the density of subducting slabs (Lin et al., 2022; Ishii et al., 2022), enhancing their negative buoyancy for further subduction into the mantle transition zone (410-660 km) or even deeper regions.

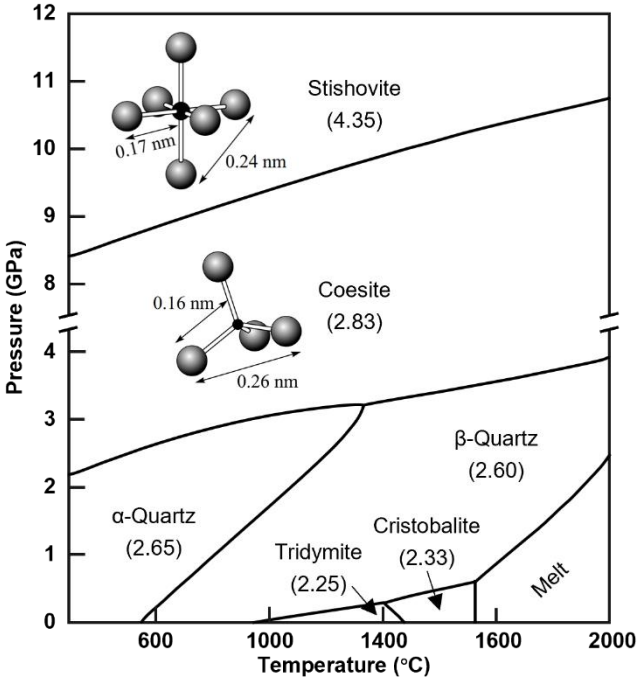

Figure 3: SiO_2 phase diagram as recommended in the reference literature (density values are indicated in brackets) (Gutzow et al., 2014). The diagram also illustrates the SiO_4 tetrahedron and SiO_6 octahedron, along with their corresponding distances.

3 Water solubility and incorporation mechanisms in stishovite

3.1 Water solubility

Research on water solubility in stishovite has primarily been conducted through high-pressure experiments (Chung and Kagi, 2002; Bromiley et al., 2006; Litasov et al., 2007; Spektor et al., 2011; Nisr et al., 2017; Lin et al., 2022; Ishii et al., 2022). Fourier transform infrared spectroscopy (FTIR) is the primary technique used to determine water content in experimental products, although results from different studies often show significant discrepancies, as detailed in Yan and Liu (2021). In this paper, we compile the experimental conditions (temperature, pressure, initial water content) and results (water and Al_2O_3 contents in stishovite products) from previous studies (Table 1).

As shown in Table 1, water solubility in stishovite is significantly influenced by temperature, pressure, and Al content, with variations more than one order of magnitude from a few ppm to a few percent. However, even under specific pressure conditions, water contents obtained by different researchers can differ by more than one order of magnitude. For example, at

https://doi.org/10.5194/egusphere-2023-2316
Preprint. Discussion started: 24 October 2023

20-25 GPa, some studies obtained 25-2700 wt. ppm water in stishovite (Litasov et al., 2007; Zhang et al., 2022), while others reported 0.5-3 wt. % water (Spektor et al., 2011; 2016). These discrepancies may partially be attributed to different water content measurement methods. Most FTIR studies obtained water contents at the ppm level, while other methods yielded water contents at the wt. % level. Additionally, the discrepancies may relate to variations in experimental conditions of temperature, and Al content in stishovite, as detailed in Sect. 4.

Table 1 Water contents in stishovite from previous studies

Temperature (°C)	Pressure (GPa)	Initial Water content (wt. %)	Al_2O_3 (wt. %)	Water content (wt. ppm)	From references
1200	10	saturated	0~1.51	7-82[a]	Pawley et al., 1993
1200-1500	15-21	saturated	0	2.5-72[b]	Bolfan-Casanova et al., 2000
1200-1400	10-15	saturated	0.612-1.341	210-759[b]	Chung and Kagi, 2002
1740-3700	30-62.9	0.2	unspecified	76-487[a]	Panero et al. 2003
1227	25	saturated	unspecified	3000*	Panero and Stixrude, 2004
1500	15	saturated	0-2.95	3-456[a]	Bromiley et al., 2006
1800	20-25	saturated	0-7.62	25-3010[b]	Litasov et al., 2007
800-1240	8-12.3	1-4	trace	53-187[c]	Thomas et al., 2009
450-550	10	saturated	<60	0.9-1.75 wt. %*	Spektor et al., 2011
627-1654	12	0-1.73	0-2.24	108-1354[b]	Yoshino et al., 2014
350-550	10	—	—	0.5-3 wt. %*	Spektor et al., 2016
450	9	—	unspecified	3.2 wt. %*	Nisr et al., 2017
950	8.4-9.1	—	unspecified	246-376[c]	Frigo et al., 2019
967-1562	32.5-52	—	0	4.6-9.9 wt. %*	Lin et al., 2020
1700	28	5	4.36	2700[b]	Ishii et al., 2022
973-1592	53-72.5	0.5-15.2	0	0.62-3.61 wt. %*	Lin et al., 2022
1700	20	saturated	3.43-5.37	2500-2700[b]	Zhang et al., 2022

Note: Most studies used Fourier transform infrared spectroscopy (FTIR) to determine water contents in stishovite with the calculation method from a. Pawley et al. (1993); b. Paterson (1982); and c. Libowitzky and Rossman (1997). * represents other methods.

3.2 Hydrogen incorporation mechanisms

Previous studies indicate two primary mechanisms for water incorporation in stishovite: (1) "hydrogarnet" substitution by $4H^+ \rightarrow Si^{4+}$; and (2) coupled substitution of H^+ and Al^{3+} for Si^{4+} ($Al^{3+} + H^+ \rightarrow Si^{4+}$). Hydrogarnet substitution is a common mechanism in pure SiO_2 stishovite. Studies by Litasov et al. (2007) have shown that stishovite can dissolve up to 5 wt. % Al_2O_3, which can further increase to 9 wt. % with the presence of water (Ono, 1999). Numerous high-pressure experiments demonstrate that Al can directly couple with H by substituting Si to increase water solubility in Al-bearing stishovite, with the

https://doi.org/10.5194/egusphere-2023-2316
Preprint. Discussion started: 24 October 2023

coupled substitution mechanism of $Al^{3+} + H^{+} \rightarrow Si^{4+}$ (Pawley et al., 1993; Chung and Kagi, 2002; Bromiley et al., 2006; Lakshtanov et al., 2007). However, Litasov et al. (2007) found that H^{+} (OH) can only co-replace Si^{4+} with up to 40% Al^{3+}, which makes the Al/H ratio in stishovite far greater than 1/1, that is, Al in stishovite is much higher than H. At this point, most Al will occupy the oxygen vacancy (O_V) and balance the charge by $2Al^{3+} + O_V^{2+} \rightarrow 2Si^{4+}$ (Pawley et al., 1993; Chung and Kagi, 2002; Litasov et al., 2007; Zhang et al., 2022).

In addition to Al^{3+}, stishovite contains minor amounts of other trivalent cations such as B^{3+}, Fe^{3+}, V^{3+}, and Cr^{3+}, which can also facilitate H incorporation into the stishovite structure by similar mechanisms as Al^{3+} (Irifune and Ringwood, 1993; Pawley et al., 1993). In summary, multiple mechanisms exist for H incorporation in stishovite with $Al^{3+} + H^{+} \rightarrow Si^{4+}$ being the most important.

4 Factors Dominating Water Solubility in Stishovite

Numerous studies demonstrate that water solubility in stishovite is primarily controlled by temperature, pressure, and Al content.

4.1 Temperature and Pressure

Numerous experiments have constrained the water solubility in Al-bearing stishovite as a function of temperature and pressure. Panero et al. (2003) showed that at 30-38 GPa, water contents in stishovite significantly increase with increasing temperature from ~100 wt. ppm at 1500 K to 400 wt. ppm at 3500 K. Litasov et al. (2007) found that at 20-25 GPa and 1000-1200 °C, H_2O contents are positively correlated with temperature, but decrease with increasing temperature from 1200-1800 °C, likely due to increased melt proportions. This can be simply explained by the fact that water preferably dissolves into the melt. Therefore, the occurrence of melt at high-temperature can significantly reduce H_2O contents in stishovite. Panero et al. (2003) showed that at 10-60 GPa, water solubility in stishovite increases with increasing pressure. Panero and Stixrude (2004) suggested that the water solubility in stishovite is ~0.3 wt. % H_2O at 25 GPa and 1500 K, and increases to 1.15 wt. % H_2O at 60 GPa, indicating increasing solubility with pressure.

By comparing previous studies, it is evident that water solubility in Al-bearing stishovite shows an overall weak positive correlation with temperature but a significant decrease when melt is present. The pressure dependence is more complex, with a positive correlation below 20 GPa but a negative correlation above 20 GPa, suggesting an optimal water solubility in stishovite at ~20 GPa (Fig. 4).

4.2 Al Content

Given that natural systems always contain some Al, its effect on water solubility in stishovite has been a focus of research. Pawley et al. (1993) found that for stishovite with >1 wt. % Al_2O_3, the H_2O content (82 wt. ppm) is ten times higher than Al-free stishovite (7 wt. ppm). Chung and Kagi (2002) showed that at 15 GPa and 1400 °C, with increasing trivalent cations

https://doi.org/10.5194/egusphere-2023-2316
Preprint. Discussion started: 24 October 2023

(mostly Al) from 0.612 wt. % to 1.341 wt. %, H_2O contents in stishovite increase from 128 wt. ppm to 536 wt. ppm. Litasov et al. (2007) obtained the maximum 3010 wt. ppm H_2O in Al-bearing stishovite (4.4 wt. % Al_2O_3) versus 16-30 wt. ppm H_2O in Al-free stishovite at 20 GPa and 1400 °C. Recent work by Ishii et al. (2022) also demonstrated the positive correlation between water solubility and Al_2O_3 content in stishovite. In contrast, Lin et al. (2022) showed decreasing water solubility in pure stishovite with increasing temperature and pressure, markedly different from Al-bearing systems. Therefore, increasing Al significantly enhances water solubility in stishovite. Statistically compiling previous data demonstrates the positive correlation between Al and water contents in stishovite (Fig. 5).

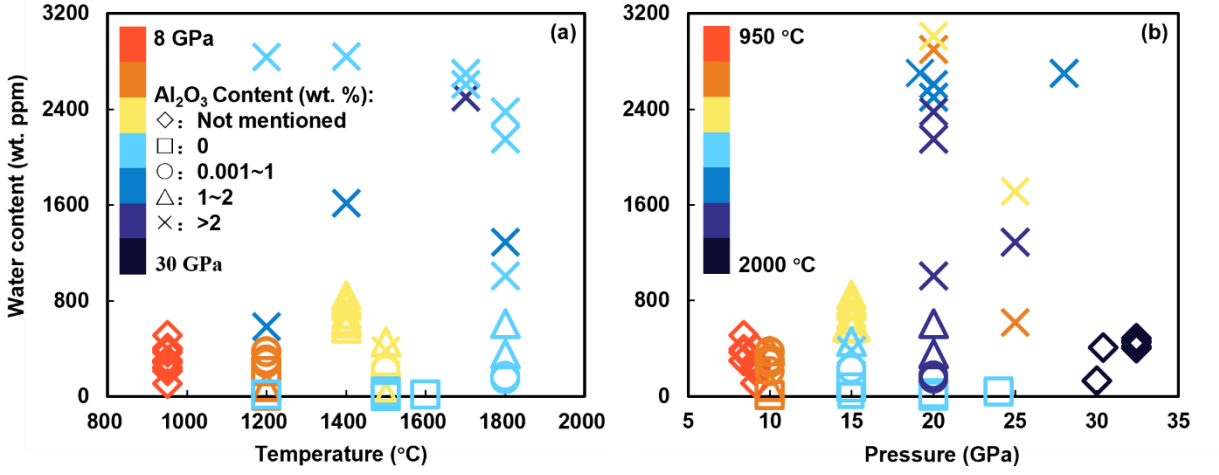

Figure 4: Previous experimental studies on water solubility in stishovite. (a) Water content versus temperature; (b) Water content versus pressure (Only FTIR data are included) (Data from Pawley et al., 1993; Bolfan-Casanova, 2000; Chung and Kagi, 2002; Panero et al., 2003; Bromiley et al., 2006; Litasov et al., 2007; Frigo et al., 2019; Ishii et al., 2022; Zhang et al., 2022)

However, the behavior of Al itself also depends on pressure and temperature. Liu et al. (2006) showed that Al solubility in stishovite decreases with pressure but increases with temperature at <2000 °C in anhydrous experiments at 15-25 GPa and 1350 °C-2150 °C. Therefore, quantitatively constraining water solubility in natural stishovite requires considering the effects of variable Al solubility under different P-T conditions. Additionally, Al expands the unit cell volume of stishovite (Litasov et al., 2007), enhancing the diffusion rate and facilitating water loss.

4.3 Other Factors

Apart from aluminum (Al), other impurity ions likely play a role in affecting water solubility in stishovite. Several studies have suggested (Ono et al., 2002; Chung and Kagi, 2002; Panero et al., 2003; Panero and Stixrude, 2004) that stishovite formed from subducted MORB (Mid-Ocean Ridge Basalt) might incorporate a variety of trivalent cations, such as Al^{3+}, Cr^{3+}, Fe^{3+}, and V^{3+}. These cations could potentially increase water content through coupled substitution. However, the work of Litasov et al. (2007) demonstrated that the H_2O content is similar between Fe-bearing stishovite (likely containing Fe^{3+}) and Al- and Fe-

https://doi.org/10.5194/egusphere-2023-2316
Preprint. Discussion started: 24 October 2023

free stishovite. Consequently, the implications of Fe^{3+}, Ti^{3+}, and other elements on water solubility in stishovite need further investigation.

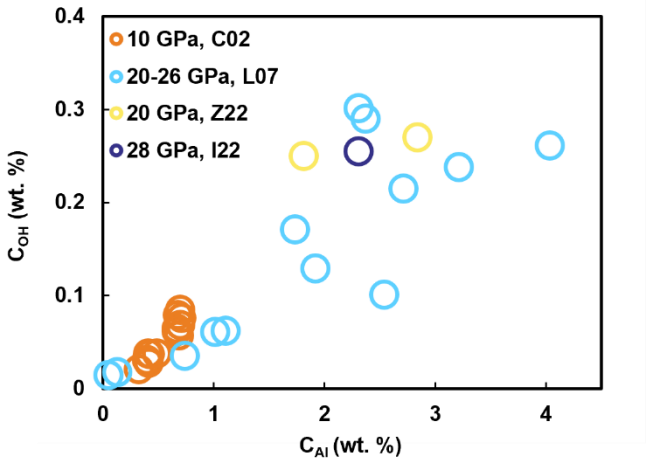

Figure 5: The correlation between H_2O and Al_2O_3 in stishovite. Data C02, L07, I22, and Z22 are from Chung and Kagi (2002), Bromiley et al. (2006), Litasov et al. (2007), Ishii et al. (2022), and Zhang et al. (2022), respectively. In Al-free stishovite, water contents range from 0.0003-0.0108 wt. % (3-108 wt. ppm), In Al-bearing stishovite, water contents increase to 0.0082-0.301 wt. % (82-3010 wt. ppm) with increasing Al.

In addition, oxygen fugacity (fO_2) stands as a crucial thermodynamic parameter that describes the oxidation state within the Earth. Its impact on water solubility within NAMs is considerable. For instance, the water solubility in olivine and orthopyroxene displays positive and negative correlations with fO_2, respectively (Yang, 2016; Liu and Yang, 2020). However, the specific influence of fO_2 on stishovite's water solubility remains to be accurately determined and requires further investigation to provide clear insights.

5 Water solubility in stishovite as a function of pressure, temperature, water fugacity, and Al content

Numerous studies have revealed that the water content in NAMs basically follows an relationship with temperature, pressure and water fugacity as shown in Eq. (1) (Kohlstedt et al., 1996; Zhao et al., 2004; Karato, 2010):

$$C_{OH} = A \cdot f_{H_2O}^{n} \cdot \ epx\left(-\frac{\Delta E + \Delta V \cdot P}{R \cdot T}\right), \quad (1)$$

where C_{OH} is the water content, A is a constant, $f_{H_2O}^{n}$ is the water fugacity, the value of n depends on the hydrogen incorporation mechanism, and ΔE and ΔV denote the energy and volume changes associated with hydrogen dissolution.

Considering the notable influence of aluminum (Al) on hydrogen solubility in stishovite ($Al^{3+} + H^{+} \rightarrow Si^{4+}$), we here propose a new model for water solubility in Al-bearing stishovite based on Eq. (2):

https://doi.org/10.5194/egusphere-2023-2316
Preprint. Discussion started: 24 October 2023

$$C_{OH}^{St} = A \cdot f_{H_2O}^{n} \cdot \ epx\left(-\frac{\Delta E + \Delta V \cdot P}{R \cdot T}\right) \cdot exp\left(\frac{B \cdot X_{Al}}{R \cdot T}\right) \quad (2)$$

In Eq. (2), C_{OH}^{St} is water solubility in Al-bearing stishovite, B is a constant, and X_{Al} is the molar fraction of Al in stishovite. Given that the dominant hydrogen incorporation mechanism corresponds to $Al^{3+} + H^{+} \rightarrow Si^{4+}$ (Pawley et al., 1993), yielding $C_{OH}^{St} \propto f_{H_2O}^{0.5}$, thus n = 0.5 (Kohlstedt et al., 1996; Karato, 2010).

To eliminate disparities arising from diverse analytical methods, we only included published FTIR data on H_2O contents in Al-bearing stishovite (Chung and Kagi, 2002; Litasov et al., 2007; Ishii et al., 2022; Zhang et al., 2022) for fitting into Eq. (2). The obtained parameters are as follows: n = 0.5, A = 0.239 ppm/bar$^{0.5}$, ΔE = -3.065 KJ/mol, ΔV = 4.29 cm^3/mol, B = 7.69 KJ/mol. Consequently, Eq. (2) can now be used to estimate the water solubility in Al-bearing stishovite across various temperature, pressure, and f_{H_2O} conditions.

We here conducted calculations to determine the water solubility in stishovite containing 3 mol. % aluminum at temperatures ranging from 800 °C to 1400 °C and pressures from 10 GPa to 40 GPa (Fig. 6). The results indicate that up to 30 GPa, water content experiences a marginal decline as temperature rises, while beyond 30 GPa, a positive correlation emerges between water content and temperature. This could be attributed to a lowered solidus under reduced pressures, leading to diminished water solubility as high-temperature, water-rich melts form. Conversely, at pressures surpassing 30 GPa, the heightened solidus counteracts the melt effect. Moreover, the solubility of water experiences a marked increase at pressures below 22 GPa to 32 GPa, followed by a decrease at pressures beyond this range, signifying an optimal solubility window. This aligns well with the overarching experimental data trend (Fig. 6b).

6 Implications for water transport to the deep Earth

Subduction zones serve as the exclusive pathway for surface water to infiltrate the Earth's deep interior. The transport and quantities of water within subducting slabs have profound impacts on surface environments, deep Earth properties and dynamics (Shillington, 2018). Existing experimental and geophysical data suggest the mantle transition zone distributes potentially water-rich regions with >1 wt. % H_2O (Pearson et al., 2014). However, the origins of this water remain a subject of debate. One perspective posits that the deep mantle has retained intrinsic wetness since Earth's formation. Alternatively, NAMs in subducting slabs may carry an amount of water to deep mantle (Peslier et al., 2017). However, it is essential to note that most hydrous minerals within subducting slabs will break down at various depths, typically having stability limits below 9 GPa, which limits the transport of water to greater mantle depths (>300 km) (Zheng et al., 2016). For instance, minerals like antigorite/phlogopite and lawsonite, which can survive to maximum depths in cold slabs, tend to dehydrate at around 300 km (Poli and Schmidt, 2002). Therefore, a fundamental question arises: can the released water from these minerals be further carried to even greater depths by NAMs?

https://doi.org/10.5194/egusphere-2023-2316
Preprint. Discussion started: 24 October 2023

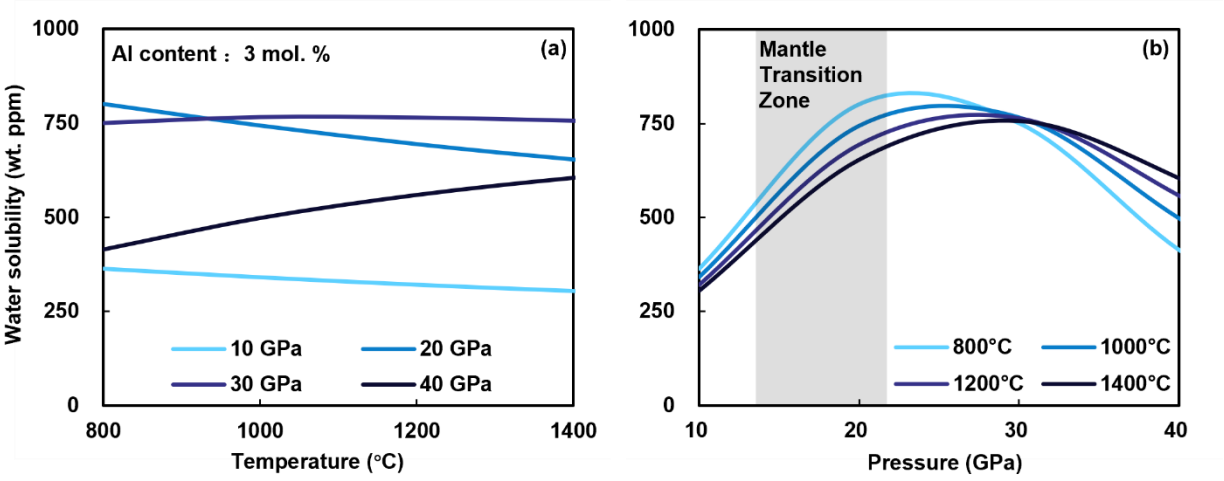

Figure 6: Water solubility in stishovite versus (a) temperature (1000-1400°C) and (b) pressure (10-40 GPa)

Existing research demonstrates that water storage capacities within upper mantle NAMs generally increase with depth (Yang and Li, 2016). Nevertheless, it is imperative to investigate how phase transitions and breakdown reactions of NAMs influence the transport of water in subducting slabs at greater depths. For instance, Gavrilenko, 2008 showed that water solubility in clinopyroxene (Cpx) decreases along a geotherm from 585 wt. ppm at 10 GPa to 135 wt. ppm at 16 GPa. Given the concurrent decomposition of Cpx from approximately 65 vol. % at 9 GPa to 0 vol. % at 16 GPa, an estimated 322 wt. ppm of water would be released from Cpx within subducted oceanic crust.

We further conducted calculations to assess the evolution of water storage capacities in major minerals within subducted Mid-Ocean Ridge Basalt (MORB) and continental sediments along a representative geotherm (Litasov and Ohtani, 2007) (Fig. 7). The results indicate that garnet and stishovite serve as primary carriers of water, with higher water storage capacities observed in subducted oceanic crust compared to sediments. In subducted MORB and continental crusts down to mantle depths, stishovite comprises 10-20 vol. % (Irifune et al., 1986; Ono et al., 2001) and >20 vol. % (Ishii et al., 2019), respectively. Our model demonstrates that stishovite water solubility increases from 612 ppm at 14 GPa to 906 ppm at 22 GPa along the geotherm. Consequently, stishovite may theoretically sequester water released from the breakdown of hydrous minerals, dehydration during mineral decomposition, and volume reduction. Additionally, stishovite water solubility peaks at 22-32 GPa (746-800 ppm at 800-1600 °C) (Fig. 6) and declines at higher pressure-temperature (P-T) conditions. Taking into account the occurrence of melts, the optimal solubility likely falls within the water-rich transition zone at pressures below 22 GPa. Consequently, stishovite emerges as a key transporter supplying water to the mantle transition zone.

https://doi.org/10.5194/egusphere-2023-2316
Preprint. Discussion started: 24 October 2023

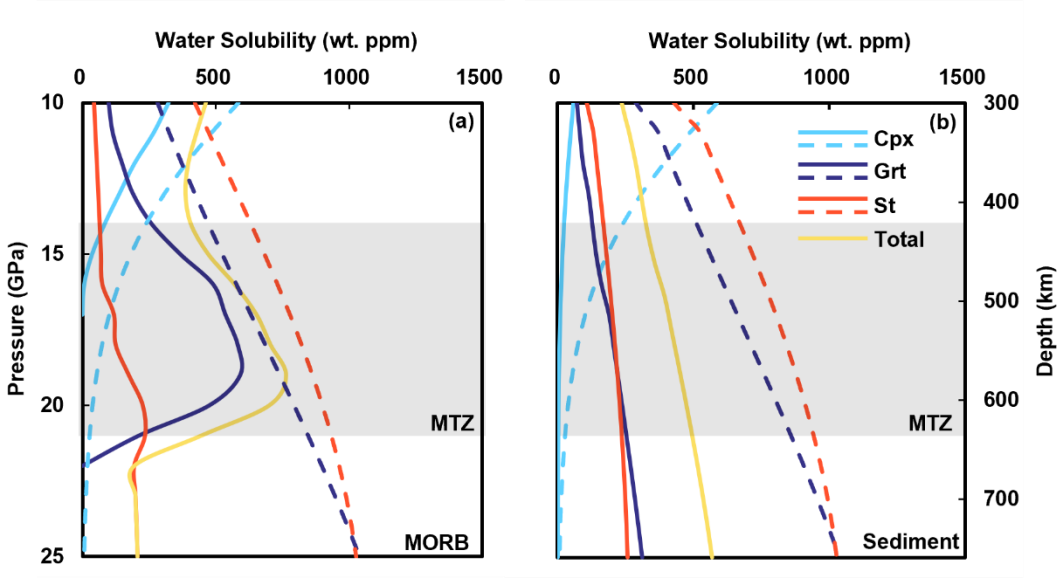

Figure 7: Evolution of water solubility in subducted crust. The hatched area represents the mantle transition zone (MTZ). WS represents water solubility. Mineral abundances follow Fig. 2; Geotherm is from (Zheng et al., 2016); Water solubility models: Grt from Yin and Kang, 2023 (in preparation), Cpx from Gavrilenko, 2008, St from this study. Dashed and solid lines represent nominal water solubilities and actual water contents considering modal fractions during subduction.

7 Conclusions and outlook

To sum up, the comprehensive review and exploration in this paper have encompassed water solubility in stishovite, hydrogen incorporation mechanisms and governing factors. We've constructed a new model for water solubility in Al-bearing stishovite and delved into stishovite's role in transporting water through subducting crust and implications for water distribution in deep Earth. The key conclusions can be as follows:

1. Water solubility in stishovite exhibits a positive correlation with Al content which increases water concentrations via coupled substitution $Al^{3+} + H^{+} \rightarrow Si^{4+}$, as well as enhances interstitial H_2O solubility by Al substitution-induced expansion of the stishovite structure.

2. The relationship between water solubility of Al-bearing stishovite and water fugacity, temperature, pressure, and Al content can be described as $C_{OH}^{St} = A \cdot f_{H_2O}^{n} \cdot epx\left(-\frac{\Delta E + \Delta V \cdot P}{R \cdot T}\right) \cdot exp\left(\frac{B \cdot X_{Al}}{R \cdot T}\right)$ with n = 0.5, A = 0.239 ppm/bar$^{0.5}$, ΔE = -3.065 KJ/mol, ΔV = 4.29 cm^3/mol, B = 7.69.

3. The calculation results from Eq. (2) demonstrate that stishovite's water solubility strongly depends on pressure, exhibiting a positive correlation below 22-32 GPa and a negative correlation above, indicating a peak solubility range at 22-32 GPa. While temperature dependence is weakly negative up to 30 GPa and weakly positive beyond.

https://doi.org/10.5194/egusphere-2023-2316
Preprint. Discussion started: 24 October 2023

4. Following a mantle geotherm, stishovite's water solubility increases from 612 wt. ppm at 14 GPa to 906 wt. ppm at 22 GPa. This suggests that stishovite can potentially absorb water released during hydrous mineral breakdown, dehydration reactions, and volume reduction, contributing to the water-rich transition zone.

However, several crucial unanswered questions persist in stishovite water solubility research: 1. The behavior of Al and its impact on water solubility across varying pressure-temperature conditions requires clarification; 2. The roles of minor elements like Fe and Ti, as well as oxygen fugacity, remain unclear; 3. Partitioning coefficients governing water distribution between stishovite, other major minerals (e.g., Cpx, Grt) and melts during slab subduction are not yet understood; 4. Equation (2) proposed in this paper needs refinement through systematic experiments conducted under controlled conditions. These issues are essential for understanding how water transports into deep Earth during subduction and require further detailed experimental and simulation-based investigations to address.

Author contribution. Mengdan Chen: Data curation, formal analysis and writing-original draft. Lei Kang: Writing - review & editing, foundation support. Danling Chen and Liang Liu: Writing - review & editing. Changxin Yin and Long Tian: Review and language modification.

Competing interest. The authors declare that they have no conflict of interest.

Acknowledgments. We are grateful to Dr. Xin Li for the discussions on Al behavior in stishovite that significantly improved this article.

Financial support. This study is supported by the Natural Science Foundation of China (Grant No. 42030307, 41972058, 42372064) and the MOST Special Fund from the State Key Laboratory of Continental Dynamics, Northwest University (Grant No. 201210233).

References

Bell, D. R., Ihinger, P. D., and Rossman, G. R.: Quantitative analysis of trace OH in garnet and pyroxenes, American Mineralogist, 80, 465–474, https://doi.org/10.2138/am-1995-5-607, 1995.

Bolfan-Casanova, N.: Water partitioning between nominally anhydrous minerals in the MgO–SiO_2–H_2O system up to 24 GPa: implications for the distribution of water in the Earth's mantle, Earth and Planetary Science Letters, 182, 209–221, https://doi.org/10.1016/S0012-821X(00)00244-2, 2000.

Bromiley, G. D., Bromiley, F. A., and Bromiley, D. W.: On the mechanisms for H and Al incorporation in stishovite, Phys Chem Minerals, 33, 613–621, https://doi.org/10.1007/s00269-006-0107-9, 2006.

https://doi.org/10.5194/egusphere-2023-2316
Preprint. Discussion started: 24 October 2023

Chao, E. C. T., Fahey, J. J., Littler, J., and Milton, D. J.: Stishovite, SiO_2, a very high pressure new mineral from Meteor Crater, Arizona, J. Geophys. Res., 67, 419–421, https://doi.org/10.1029/JZ067i001p00419, 1962.

Chung, J. I. and Kagi, H.: High concentration of water in stishovite in the MORB system, Geophys. Res. Lett., 29, 2020, https://doi.org/10.1029/2002GL015579, 2002.

Frigo, C., Stalder, R., and Ludwig, T.: OH defects in coesite and stishovite during ultrahigh-pressure metamorphism of continental crust, Phys Chem Minerals, 46, 77–89, https://doi.org/10.1007/s00269-018-0987-5, 2019.

Gavrilenko, P.: Water solubility in diopside, Ph.D. thesis, Universität Bayreuth, Germany, 2008.

Gutzow, I., Pascova, R., Jordanov, N., Gutzov, S., Penkov, I., Markovska, I., Schmelzer, J. W. P., and Ludwig, F. P.: Crystalline and Amorphous Modifications of Silica: Structure, Thermodynamic Properties, Solubility, and Synthesis, in: Glass, edited by: Schmelzer, J. W. P., De Gruyter, 137–196, https://doi.org/10.1515/9783110298581.137, 2014.

Holtstam, D., Broman, C., Söderhielm, J., and Zetterqvist, A.: First discovery of stishovite in an iron meteorite, Meteoritics & Planetary Science, 38, 1579–1583, https://doi.org/10.1111/j.1945-5100.2003.tb00002.x, 2003.

Irifune, T. and Ringwood, A. E.: Phase transformations in subducted oceanic crust and buoyancy relationships at depths of 600–800 km in the mantle, Earth and Planetary Science Letters, 117, 101–110, https://doi.org/10.1016/0012-821X(93)90120-X, 1993.

Irifune, T., Sekine, T., Ringwood, A. E., and Hibberson, W. O.: The eclogite-garnetite transformation at high pressure and some geophysical implications, Earth and Planetary Science Letters, 77, 245–256, https://doi.org/10.1016/0012-821X(86)90165-2, 1986.

Irifune, T., Ringwood, A. E., and Hibberson, W. O.: Subduction of continental crust and terrigenous and pelagic sediments: an experimental study, Earth and Planetary Science Letters, 126, 351–368, https://doi.org/10.1016/0012-821X(94)90117-1, 1994.

Ishii, T., Kojitani, H., and Akaogi, M.: High-pressure phase transitions and subduction behavior of continental crust at pressure–temperature conditions up to the upper part of the lower mantle, Earth and Planetary Science Letters, 357–358, 31–41, https://doi.org/10.1016/j.epsl.2012.09.019, 2012.

Ishii, T., Kojitani, H., and Akaogi, M.: Phase Relations of Harzburgite and MORB up to the Uppermost Lower Mantle Conditions: Precise Comparison with Pyrolite by Multisample Cell High-Pressure Experiments with Implication to Dynamics of Subducted Slabs, J. Geophys. Res. Solid Earth, 124, 3491–3507, https://doi.org/10.1029/2018JB016749, 2019.

Ishii, T., Criniti, G., Ohtani, E., Purevjav, N., Fei, H., Katsura, T., and Mao, H.: Superhydrous aluminous silica phases as major water hosts in high-temperature lower mantle, Proc. Natl. Acad. Sci. U.S.A., 119, e2211243119, https://doi.org/10.1073/pnas.2211243119, 2022.

Johnson, E. A.: Water in Nominally Anhydrous Crustal Minerals: Speciation, Concentration, and Geologic Significance, Reviews in Mineralogy and Geochemistry, 62, 117–154, https://doi.org/10.2138/rmg.2006.62.6, 2006.

https://doi.org/10.5194/egusphere-2023-2316
Preprint. Discussion started: 24 October 2023

Kaminsky, F.: Mineralogy of the lower mantle: A review of 'super-deep' mineral inclusions in diamond, Earth-Science Reviews, 110, 127–147, https://doi.org/10.1016/j.earscirev.2011.10.005, 2012.

Karato, S.: Rheology of the deep upper mantle and its implications for the preservation of the continental roots: A review, Tectonophysics, 481, 82–98, https://doi.org/10.1016/j.tecto.2009.04.011, 2010.

Keskar, N. R., Troullier, N., Martins, J. L., and Chelikowsky, J. R.: Structural properties of SiO_2 in the stishovite structure, Phys. Rev. B, 44, 4081–4088, https://doi.org/10.1103/PhysRevB.44.4081, 1991.

Kohlstedt, D. L., Keppler, H., and Rubie, D. C.: Solubility of water in the α, β and γ phases of $(Mg,Fe)_2SiO_4$, Contributions to Mineralogy and Petrology, 123, 345–357, https://doi.org/10.1007/s004100050161, 1996.

Lakshtanov, D. L., Litasov, K. D., Sinogeikin, S. V., Hellwig, H., Li, J., Ohtani, E., and Bass, J. D.: Effect of Al^{3+} and H^+ on the elastic properties of stishovite, American Mineralogist, 92, 1026–1030, https://doi.org/10.2138/am.2007.2294, 2007.

Libowitzky, E.: The Structure of Hydrous Species in Nominally Anhydrous Minerals: Information from Polarized IR Spectroscopy, Reviews in Mineralogy and Geochemistry, 62, 29–52, https://doi.org/10.2138/rmg.2006.62.2, 2006.

Libowitzky, E. and Rossman, G. R.: An IR absorption calibration for water in minerals, American Mineralogist, 82, 1111–1115, https://doi.org/10.2138/am-1997-11-1208, 1997.

Lin, Y., Hu, Q., Meng, Y., Walter, M., and Mao, H.-K.: Evidence for the stability of ultrahydrous stishovite in Earth's lower mantle, Proc. Natl. Acad. Sci. U.S.A., 117, 184–189, https://doi.org/10.1073/pnas.1914295117, 2020.

Lin, Y., Hu, Q., Walter, M. J., Yang, J., Meng, Y., Feng, X., Zhuang, Y., Cohen, R. E., and Mao, H.-K.: Hydrous SiO_2 in subducted oceanic crust and H_2O transport to the core-mantle boundary, Earth and Planetary Science Letters, 594, 117708, https://doi.org/10.1016/j.epsl.2022.117708, 2022.

Litasov, K. D. and Ohtani, E.: Effect of water on the phase relations in Earth's mantle and deep water cycle, in: Advances in High-Pressure Mineralogy, Geological Society of America, https://doi.org/10.1130/2007.2421(08), 2007.

Litasov, K. D., Kagi, H., Shatskiy, A., Ohtani, E., Lakshtanov, D. L., Bass, J. D., and Ito, E.: High hydrogen solubility in Al-rich stishovite and water transport in the lower mantle, Earth and Planetary Science Letters, 262, 620–634, https://doi.org/10.1016/j.epsl.2007.08.015, 2007.

Liu, H. and Yang, X.: Solubility of hydroxyl groups in pyroxenes: Effect of oxygen fugacity at 0.2–3 GPa and 800–1200 °C, Geochimica et Cosmochimica Acta, 286, 355–379, https://doi.org/10.1016/j.gca.2020.07.034, 2020.

Liu, L., Zhang, J., Green, H. W., Jin, Z., and Bozhilov, K. N.: Evidence of former stishovite in metamorphosed sediments, implying subduction to > 350 km, Earth and Planetary Science Letters, 263, 180–191, https://doi.org/10.1016/j.epsl.2007.08.010, 2007.

Liu, L., Zhang, J. F., Cao, Y. T., Green, H. W., Yang, W. Q., Xu, H. J., Liao, X. Y., and Kang, L.: Evidence of former stishovite in UHP eclogite from the South Altyn Tagh, western China, Earth and Planetary Science Letters, 484, 353–362, https://doi.org/10.1016/j.epsl.2017.12.023, 2018.

https://doi.org/10.5194/egusphere-2023-2316
Preprint. Discussion started: 24 October 2023

Liu, X., Nishiyama, N., Sanehira, T., Inoue, T., Higo, Y., and Sakamoto, S.: Decomposition of kyanite and solubility of Al_2O_3 in stishovite at high pressure and high temperature conditions, Phys Chem Minerals, 33, 711–721, https://doi.org/10.1007/s00269-006-0122-x, 2006.

Liu, X. W., Xie, Z. J., Wang, L., Xu, W., and Jin, Z. M.: Water incorporation in garnets from ultrahigh pressure eclogites at Shuanghe, Dabieshan, Mineral. mag., 80, 959–975, https://doi.org/10.1180/minmag.2016.080.034, 2016.

Magni, V., Bouilhol, P., and Van Hunen, J.: Deep water recycling through time, Geochem. Geophys. Geosyst., 15, 4203–4216, https://doi.org/10.1002/2014GC005525, 2014.

Nisr, C., Shim, S. H., Leinenweber, K., and Chizmeshya, A.: Raman spectroscopy of water-rich stishovite and dense high-pressure silica up to 55 GPa, American Mineralogist, 102, 2180–2189, https://doi.org/10.2138/am-2017-5944, 2017.

Ono, S.: High temperature stability limit of phase egg, $AlSiO_3(OH)$, Contributions to Mineralogy and Petrology, 137, 83–89, https://doi.org/10.1007/s004100050583, 1999.

Ono, S., Ito, E., and Katsura, T.: Mineralogy of subducted basaltic crust (MORB) from 25 to 37 GPa, and chemical heterogeneity of the lower mantle, Earth and Planetary Science Letters, 190, 57–63, https://doi.org/10.1016/S0012-821X(01)00375-2, 2001.

Ono, S., Suto, T., Hirose, K., Kuwayama, Y., Komabayashi, T., and Kikegawa, T.: Equation of state of Al-bearing stishovite to 40 GPa at 300 K, American Mineralogist, 87, 1486–1489, https://doi.org/10.2138/am-2002-1026, 2002.

Ono, S., Kikegawa, T., Higo, Y., and Tange, Y.: Precise determination of the phase boundary between coesite and stishovite in SiO_2, Physics of the Earth and Planetary Interiors, 264, 1–6, https://doi.org/10.1016/j.pepi.2017.01.003, 2017.

Panero, W. R. and Stixrude, L. P.: Hydrogen incorporation in stishovite at high pressure and symmetric hydrogen bonding in δ-AlOOH, Earth and Planetary Science Letters, 221, 421–431, https://doi.org/10.1016/S0012-821X(04)00100-1, 2004.

Panero, W. R., Benedetti, L. R., and Jeanloz, R.: Transport of water into the lower mantle: Role of stishovite: TRANSPORT OF WATER INTO THE LOWER MANTLE, J. Geophys. Res., 108, https://doi.org/10.1029/2002JB002053, 2003.

Paterson, M. S.: The determination of hydroxyl by infrared absorption in quartz, silicate glasses and similar materials, bulmi, 105, 20–29, https://doi.org/10.3406/bulmi.1982.7582, 1982.

Pawley, A. R., McMillan, P. F., and Holloway, J. R.: Hydrogen in Stishovite, with Implications for Mantle Water Content, Science, 261, 1024–1026, https://doi.org/10.1126/science.261.5124.1024, 1993.

Pearson, D. G., Brenker, F. E., Nestola, F., McNeill, J., Nasdala, L., Hutchison, M. T., Matveev, S., Mather, K., Silversmit, G., Schmitz, S., Vekemans, B., and Vincze, L.: Hydrous mantle transition zone indicated by ringwoodite included within diamond, Nature, 507, 221–224, https://doi.org/10.1038/nature13080, 2014.

Peslier, A. H., Schönbächler, M., Busemann, H., and Karato, S.-I.: Correction to: Water in the Earth's Interior: Distribution and Origin, Space Sci Rev, 212, 811–811, https://doi.org/10.1007/s11214-017-0420-2, 2017.

Petersen, S. E., Hoisch, T. D., and Porter, R. C.: Assessing the Role of Water in Alaskan Flat-Slab Subduction, Geochem Geophys Geosyst, 22, e2021GC009734, https://doi.org/10.1029/2021GC009734, 2021.

https://doi.org/10.5194/egusphere-2023-2316
Preprint. Discussion started: 24 October 2023

Poli, S. and Schmidt, M. W.: Petrology of Subducted Slabs, Annu. Rev. Earth Planet. Sci., 30, 207–235, https://doi.org/10.1146/annurev.earth.30.091201.140550, 2002.

Rossman, G. R.: Studies of OH in nominally anhydrous minerals, Phys Chem Minerals, 23, https://doi.org/10.1007/BF00207777, 1996.

Shillington, D. J.: Water takes a deep dive into an oceanic tectonic plate, Nature, 563, 335–336, https://doi.org/10.1038/d41586-018-07335-8, 2018.

Smith, E. M., Shirey, S. B., Richardson, S. H., Nestola, F., Bullock, E. S., Wang, J., and Wang, W.: Blue boron-bearing diamonds from Earth's lower mantle, Nature, 560, 84–87, https://doi.org/10.1038/s41586-018-0334-5, 2018.

Spektor, K., Nylen, J., Stoyanov, E., Navrotsky, A., Hervig, R. L., Leinenweber, K., Holland, G. P., and Häussermann, U.: Ultrahydrous stishovite from high-pressure hydrothermal treatment of SiO_2, Proc. Natl. Acad. Sci. U.S.A., 108, 20918–20922, https://doi.org/10.1073/pnas.1117152108, 2011.

Spektor, K., Nylen, J., Mathew, R., Edén, M., Stoyanov, E., Navrotsky, A., Leinenweber, K., and Häussermann, U.: Formation of hydrous stishovite from coesite in high-pressure hydrothermal environments, American Mineralogist, 101, 2514–2524, https://doi.org/10.2138/am-2016-5609, 2016.

Thomas, R., Davidson, P., Rericha, A., and Recknagel, U.: Discovery of Stishovite in the Prismatine-Bearing Granulite from Waldheim, Germany: A Possible Role of Supercritical Fluids of Ultrahigh-Pressure Origin, Geosciences, 12, 196, https://doi.org/10.3390/geosciences12050196, 2022.

Thomas, S.-M., Koch-Müller, M., Reichart, P., Rhede, D., Thomas, R., Wirth, R., and Matsyuk, S.: IR calibrations for water determination in olivine, r-GeO_2, and SiO_2 polymorphs, Phys Chem Minerals, 36, 489–509, https://doi.org/10.1007/s00269-009-0295-1, 2009.

Walter, M. J.: Water transport to the core–mantle boundary, National Science Review, 8, nwab007, https://doi.org/10.1093/nsr/nwab007, 2021.

Wu, Y., Fei, Y., Jin, Z., and Liu, X.: The fate of subducted Upper Continental Crust: An experimental study, Earth and Planetary Science Letters, 282, 275–284, https://doi.org/10.1016/j.epsl.2009.03.028, 2009.

Xia, Q. K., Chen, D. G., Deloule, E., and Zhi, X. C.: Hydrogen isotopic compositions of mantle-derived megacrysts from cenozoic basalts, Eastern China, Chin.Sci.Bull., 43, 146–146, https://doi.org/10.1007/BF02891632, 1998.

Yan, B., Liu, S., Chastain, M. L., Yang, S., and Chen, J.: A new FTIR method for estimating the firing temperature of ceramic bronze-casting moulds from early China, Sci Rep, 11, 3316, https://doi.org/10.1038/s41598-021-82806-z, 2021.

Yang, X.: Effect of oxygen fugacity on OH dissolution in olivine under peridotite-saturated conditions: An experimental study at 1.5–7 GPa and 1100–1300 °C, Geochimica et Cosmochimica Acta, 173, 319–336, https://doi.org/10.1016/j.gca.2015.11.007, 2016.

Yang, X. and Li, Y.: High-P/T experimental studies and water in the silicate mantle, Sci. China Earth Sci., 59, 683–695, https://doi.org/10.1007/s11430-015-5241-0, 2016.

https://doi.org/10.5194/egusphere-2023-2316
Preprint. Discussion started: 24 October 2023

Yin, C. X. and Kang, L.: Water in eclogite from subduction zone: a short review (in Chinese), Geological Journal of China Universities, 2023 (in preparation).

Yoshino, T., Shimojuku, A., and Li, D.: Electrical conductivity of stishovite as a function of water content, Physics of the Earth and Planetary Interiors, 227, 48–54, https://doi.org/10.1016/j.pepi.2013.12.003, 2014.

Zhang, Y., Fu, S., Karato, S., Okuchi, T., Chariton, S., Prakapenka, V. B., and Lin, J.: Elasticity of Hydrated Al-Bearing Stishovite and Post-Stishovite: Implications for Understanding Regional Seismic V_S Anomalies Along Subducting Slabs in the Lower Mantle, JGR Solid Earth, 127, https://doi.org/10.1029/2021JB023170, 2022.

Zhao, Y.H., Ginsberg, S. B., and Kohlstedt, D. L.: Solubility of hydrogen in olivine: dependence on temperature and iron content, Contributions to Mineralogy and Petrology, 147, 155–161, https://doi.org/10.1007/s00410-003-0524-4, 2004.

Zheng, Y., Chen, R., Xu, Z., and Zhang, S.: The transport of water in subduction zones, Sci. China Earth Sci., 59, 651–682, https://doi.org/10.1007/s11430-015-5258-4, 2016.